

Current-driven magnetic domain wall motion in heterostructure films

Rui Fu(付瑞), Jiwen Chen(陈集文), Zichang Huang(黄子畅), Jingyi Guan(管璟一), Zidong Wang(王子东), and Yan Zhou(周艳)

Citation: Chin. Phys. B, 2025, 34 (**12**): 127502. DOI: 10.1088/1674-1056/ade4ad
http://cpb.iphy.ac.cn; http://iopscience.iop.org/cpb

What follows is a list of articles you may be interested in

Directly tunable magnon frequency comb effect based on domain wall

Xiaoxue Yang(杨霄雪), Huiting Li(李慧婷), Xue-Feng Zhang(张雪枫), Xiao-Ping Ma(马晓萍), Je-Ho Shim(沈帝虎), Yingjiu Jin(金迎九), and Hong-Guang Piao(朴红光)

Chin. Phys. B, 2025, 34 (**10**): 107507. DOI: 10.1088/1674-1056/ade856

Multi-segmented nanowires for vortex magnetic domain wall racetrack memory

M Al Bahri, M Al Hinaai, and T Al Harthy

Chin. Phys. B, 2023, 32 (**12**): 127508. DOI: 10.1088/1674-1056/acca0a

Effect of CeO_2 doping on the coercivity of 2:17 type SmCo magnets

Xiao-Lei Gao(高晓磊), Zhuang Liu(刘壮), Guang-Qing Wang(王广庆), Chao-Qun Zhu(竺超群), Wen-Xin Cheng(程文鑫), Ming-Xiao Zhang(张明晓), Xin-Cai Liu(刘新才), Ren-Jie Chen(陈仁杰), and A-Ru Yan(闫阿儒)

Chin. Phys. B, 2023, 32 (**9**): 097504. DOI: 10.1088/1674-1056/acaa24

Asymmetric dynamic behaviors of magnetic domain wall in trapezoid-cross-section nanostrip

Xiao-Ping Ma(马晓萍), Hong-Guang Piao(朴红光), Lei Yang(杨磊), Dong-Hyun Kim, Chun-Yeol You, Liqing Pan(潘礼庆)

Chin. Phys. B, 2020, 29 (**9**): 097502. DOI: 10.1088/1674-1056/aba09a

Model of hybrid interfacial domain wall in ferromagnetic/antiferromagnetic bilayers

Zhang Wen (章文), Zhai Ya (翟亚), Lu Mu (鹿牧), You Biao (游彪), Zhai Hong-Ru (翟宏如), Caroline G Morgan

Chin. Phys. B, 2015, 24 (**4**): 047502. DOI: 10.1088/1674-1056/24/4/047502

Current-driven magnetic domain wall motion in heterostructure films

Rui Fu(付瑞), Jiwen Chen(陈集文), Zichang Huang(黄子畅),
Jingyi Guan(管璟一), Zidong Wang(王子东), and Yan Zhou(周艳)†

School of Science and Engineering, The Chinese University of Hong Kong, Shenzhen 518172, *China*

(Received 26 February 2025; revised manuscript received 13 June 2025; accepted manuscript online 16 June 2025)

With the rise of big data, the increasing volume of information has raised significant demands on data storage technologies, presenting various challenges to current information storage solutions. Consequently, finding more efficient and higher-capacity methods for data storage has become crucial. In comparison to conventional semiconductor random access memory, magnetic random access memory (MRAM), which has been progressively developed in recent years, shows promise as a candidate for the next generation of information storage due to its notable advantages, including non-volatility, high density, stability, low power consumption, and resistance to radiation. Among the MRAM variants, spin–orbit torque magnetic random access memory (SOT-MRAM) exhibits considerable potential for advancement. Utilizing a vertical magnetized thin film structure made up of heavy metal and ferromagnetic metal, SOT-MRAM leverages the strong spin–orbit coupling effect of the heavy metal to convert the flow of charge into pure spin flow. This process also allows for the injection of spin accumulation from the interface into the adjacent magnetic layer through mechanisms such as the spin Hall effect and the Rashba effect, ultimately applying spin–orbit torque to manipulate the magnetic moment of the magnetic layer, facilitating its reversal. This paper primarily investigates the physical mechanisms underlying the motion of magnetic domain walls driven by current-induced spin–orbit moments in vertically magnetized heterostructures. Utilizing a magneto-optical Kerr microscope to observe the movement of the magnetic domain walls, the study analyzes and compares the velocity behaviors of the domain walls across different cobalt thicknesses. These investigations offer valuable design insights for applications involving track memory driven by spin–orbit moments.

Keywords: magnetic domain wall, spin–orbit torque, magneto-optical Kerr microscope, track memory

PACS: 75.78.–n

DOI: 10.1088/1674-1056/ade4ad **CSTR:** 32038.14.CPB.ade4ad

1. Introduction

Magnetic heterostructure films, owing to their ultra-thin nature, exhibit a range of intriguing and often unique physical effects at the interface, positioning them as promising candidates for advanced spintronic applications. Among these, the phenomenon of compensated ferrimagnetism has been observed in thin-film heterostructure systems. However, a comprehensive understanding of the relationship between ferrimagnetism and film thickness remains incomplete, and the electrical control of ultrafast domain wall motion is yet to be realized. This work aims to deepen the understanding of the impact of magnetic thin-film thickness on domain wall dynamics and contribute to the development of novel systems for racetrack memory, based on the motion of domain walls, thus guiding the future evolution of spintronic devices.

In vertically magnetized heterostructures composed of heavy metals and ferromagnetic materials, strong spin–orbit coupling induces an additional asymmetric exchange interaction at the interface, known as the Dzyaloshinskii–Moriya interaction (DMI).[1] This interaction fosters the emergence of complex spin textures in the magnetic layer, including chiral magnetic domain walls and topologically protected states.[2,3] For example, Yu *et al*. (2014) demonstrated that DMI stabilizes chiral domain walls in ultrathin ferromagnetic films, providing a robust mechanism for efficient domain wall motion.[6] Similarly, Murray *et al*. (2019) emphasized the importance of such spin textures in achieving high-speed domain wall motion, which is critical for the development of memory devices reliant on domain wall dynamics.[7]

Among these spin textures, the Néel domain wall, characterized by a fixed chirality, can be driven by current-induced spin–orbit torques, thus enabling high-speed domain wall motion: an essential requirement for next-generation racetrack memory devices based on domain wall motion.[8,9] The work of Razavi *et al*. (2017) and Lau *et al*. (2016) has highlighted the potential of current-induced torques in generating highly efficient domain wall motion, advancing the development of high-performance spintronic devices.[10,11] The stabilization of chiral domain walls within systems exhibiting interface DMI facilitates their motion at high velocities, a crucial factor for the realization of fast, energy-efficient memory technologies, as demonstrated by Miron *et al*. (2011) and Emori *et al*. (2012).[24,25]

†Corresponding author. E-mail: zhouyan@cuhk.edu.cn

© 2025 Chinese Physical Society and IOP Publishing Ltd. All rights, including for text and data mining, AI training, and similar technologies, are reserved.

The possibility of high-speed, current-driven domain wall motion has also been extensively studied in ultrathin films with perpendicular magnetic anisotropy. Moore *et al*. (2008) demonstrated that the inclusion of DMI can lead to extremely high domain wall velocities in ultrathin Pt/Co/AlO_x wires, presenting a promising pathway for the development of faster memory devices.[22] Moreover, Miron *et al*. (2009) showed that domain wall manipulation via spin torque can be employed as an effective method for controlling domain walls at the nanoscale.[23] These pioneering studies laid the foundation for controlling domain wall dynamics using electrical currents, a crucial step in the development of spintronic memory technologies.

2. Results and discussion

2.1. Sample preparation

We use rare earth/transition metal (RE/TM) of Co/Gd heterostructure in our experiments and it shows strongly antiferromagnetic exchange coupling. The stacking of multilayers involving ferrimagnets Ta (5 nm)/Pt (5 nm)/Co (0.5 nm)/Gd (0.6 nm–1.4 nm)/Pt (5 nm) is shown in Fig. 1 below. In this experiment, samples of heterostructure thin films were prepared by ultra-high vacuum magnetron sputtering, and then the above films were etched into Hall bar device structure by laser direct writing instrument and argon ion etching equipment. By changing the relative deposition rate, the thickness of Gd in these heterostructures can be changed. All films show perpendicular magnetic anisotropy (PMA). Note that 5-nm thick Ta is used as the seed layer under Pt/Co/Gd stripes and 5-nm thick Pt layer is also used as the cover layer to prevent environmental oxidation.

2.2. Under an out-of-plane magnetic field

Figure 1(a) shows an optical image of the long microstructured strip of length 100 μm and width 10 μm. We further compare the current-induced domain wall (DW) motion under the magnetic field along the x-axis. Before the microsecond current pulse is applied to a racetrack-like device, the nucleation of DW is realized by the following steps: In order to control the motion of magnetic domain walls (DWs), a positive or negative magnetic field is initially applied to achieve a saturation state within the magnetic domain wall. Subsequently, the magnetic field strength is reduced to transition into a reverse and unsaturated magnetic field, thereby facilitating the movement of the magnetic domain wall toward the device's racetrack region. Additionally, an external magnetic field is established, and microsecond-duration current pulses are applied to enhance the control of DW dynamics.

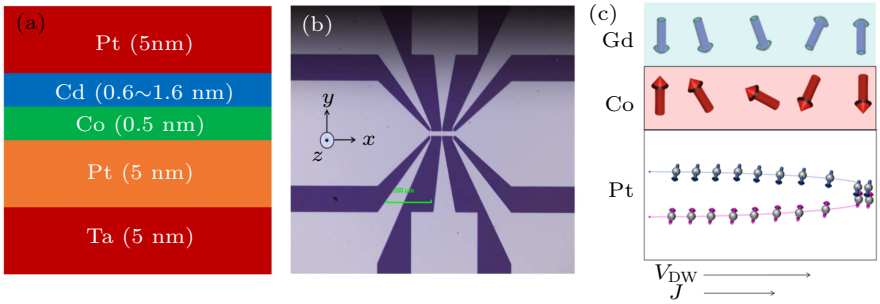


Fig. 1. (a) Schematic diagram of stacking sequence of samples and (b) simulated images of microstrip devices used to study DW motion. The out-of-plane magnetic field is in the z direction, and the motion of the magnetic domain wall is reversed along x axis. (c) Schematic diagram of a DW in ferrimagnetic Pt|Co|Gd in the presence of a current j. Arrows and colors in the Co|Gd layers represent the direction of the local magnetic moment, with the thickness of the arrows being the magnitude of the moment.

It is crucial to note that if the magnitude of the external magnetic field is below the pinning field threshold, the motion of the domain walls will be inhibited, as the walls remain immobilized due to local energy barriers. The dynamics of magnetic domains and their associated walls are investigated using a magneto-optical Kerr effect (MOKE) microscope, which allows for real-time imaging of their motion and behavior. This advanced imaging technique is instrumental in studying the fundamental mechanisms governing magnetic domain dynamics and has significant implications for applications in fields such as spintronics and high-density memory technologies, including magnetic random access memory (MRAM).

In Fig. 2(b) following a similar nucleation method, a pair of left-handed Néel DWs are stable in the Ta/Pt/Co/Gd/Pt stack, in which the interface inversion symmetry breaking provides a strong interface DMI, and high spin–orbit torque (SOT) efficiency is achieved. Cobalt, as a transition metal, possesses a 3d lone pair, while the magnetic moment of the rare earth element gadolinium is predominantly attributed to its unpaired 4f electrons. The arrangement of the magnetic moments of neighboring atoms in opposite orientations results in a net magnetic moment approaching zero, thus yielding an antiferromagnetic coupling effect within the system.

In magnetic materials, the spin–orbit coupling (SOC) phenomenon can significantly enhance the efficiency of converting spin-polarized currents. When a spin-polarized current traverses the material, it can exert influence over angular momentum, thereby facilitating the movement of magnetic do-

main walls. The robust nature of SOC accelerates the dynamics of the magnetic domain walls in response to the applied current.

Cobalt, being a ferromagnetic material, exhibits a thin-layer structure that allows its magnetization direction to be readily influenced by the spin orbital moment. The incorporation of a gadolinium layer can further augment the SOC effect at the interface, resulting in an enhanced spin–orbit moment.

At the interface between a heavy metal (such as platinum) with strong SOC characteristics and a magnetic layer (such as cobalt), the generation of transverse spin current is facilitated by the spin Hall effect (SHE). As the current flows through the platinum layer, these spin currents can induce an SOT within the cobalt layer, ultimately leading to magnetization reversal. This interplay between the materials underscores the critical role of SOC in manipulating magnetic properties for advanced applications in spintronics.

Figure 2 presents a series of MOKE images captured subsequent to the application of continuous current pulses of a specified duration. In this context, the rightward direction is designated as the positive direction of the DW velocity. The average DW velocity is determined by dividing the total displacement of the domain wall by the cumulative duration of the applied pulse sequence. Each data set is obtained through three independent repetitions, and the corresponding average value is calculated to ensure accuracy and reliability in the results. This comprehensive approach enables a robust assessment of the dynamics of domain wall motion under continuous current stimulation.

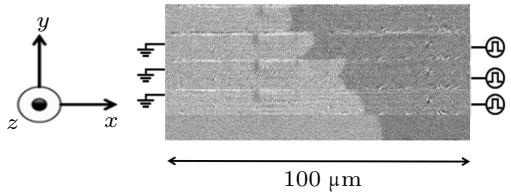


Fig. 2. Only applying pulse current without applying magnetic field can also drive the motions of magnetic domain wall. Black and gray areas represent downward and upward magnetic domain walls, respectively.

After the continuous current pulse is applied, images of DW displacement are obtained in 10-μm-wide and 100-μm-long stripes by MOKE microscope.

Figure 3 depicts the relationship between the velocity of the magnetic domain wall and the strength of the applied magnetic field at various current densities. A noteworthy finding is that the velocity of the magnetic domain wall exhibits a proportional relationship with the intensity of the applied magnetic field. Specifically, as the magnetic field strength increases, the velocity of the magnetic domain wall correspondingly escalates, thereby revealing a clear linear correlation. Furthermore, it is important to highlight that the direction of the magnetic domain wall's movement aligns with the direction of the applied current.

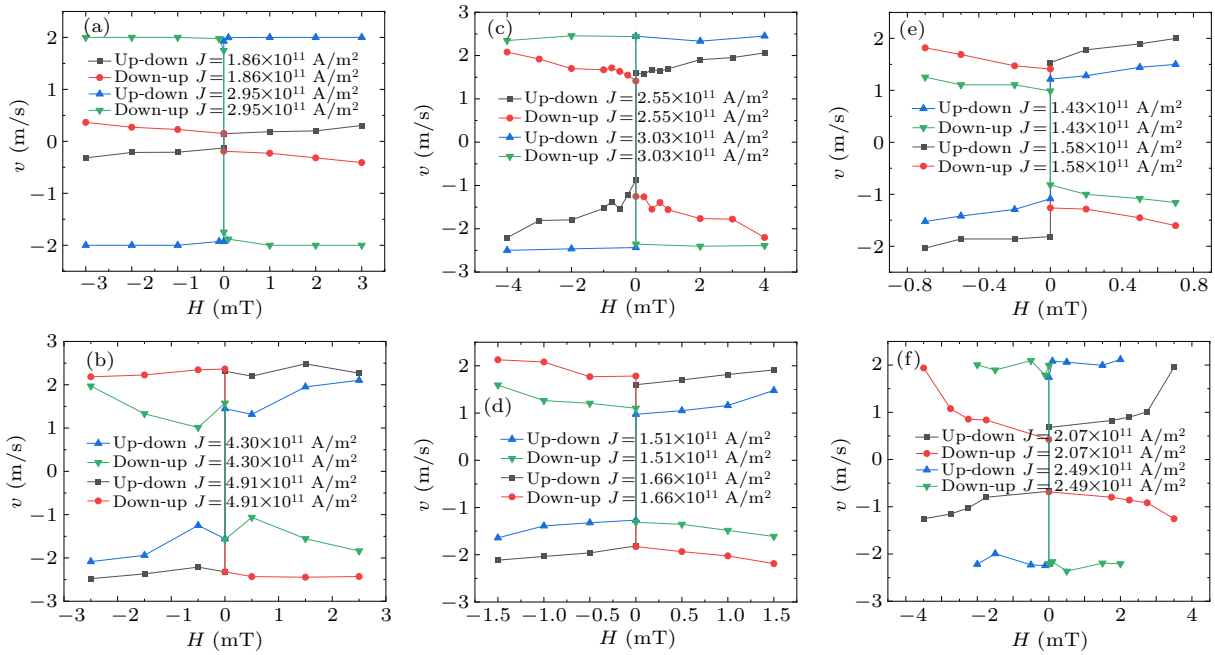


Fig. 3. DW velocity as a function of the applied out-of plane field (H) along the x-direction at a certain current density in a 10-μm-wide strip device made of Gd 0.6 nm, 0.8 nm, 1.0 nm, 1.1 nm, 1.3 nm, Gd 1.4 nm, respectively.

As the thickness of Gd is gradually increased, it becomes evident that achieving a consistent magnetic domain wall velocity initially requires an increase in current density. The maximum current density occurs at a thickness of 0.9 nm. Beyond this point, as the thickness continues to rise, the required current density begins to decrease. Notably, at a thickness of 1.1 nm, only the minimum current density is sufficient to maintain the desired speed.

Correspondingly, figure 4(b) illustrates that Gd at a thickness of 1.1 nm exhibits the steepest slope in the change of

velocity, suggesting that this thickness is indicative of ferrimagnetic compensation. This condition appears to correspond to an optimal regime for the motion of magnetic domain walls, facilitating the fastest dynamics. Therefore, under controlled current density conditions, the velocity of the magnetic domain wall demonstrates a non-monotonic behavior, initially decreasing before subsequently increasing, reaching its peak velocity at a thickness of 1.1 nm.

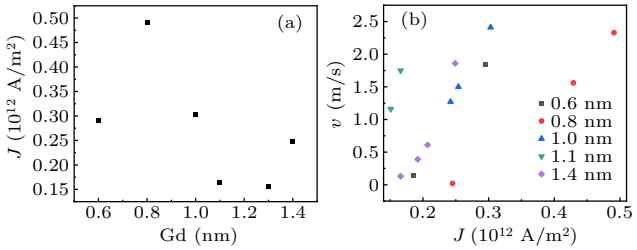


Fig. 4. (a) When the thickness of Gd is 1.6 nm, the minimum current density is needed to achieve the same speed of 2 m/s, so it is inferred that the thickness at this time is the thickness compensation point. (b) Scatter diagram of the relationship between different Gd thickness, current density, and magnetic domain wall motion velocity under zero magnetic field.

2.3. Analysis of effect on thickness-dependent spin angular momentum

Cobalt (Co) and gadolinium (Gd) represent a class of transition metals and rare earth elements, respectively, each exhibiting distinct magnetic properties characterized by their magnetic moments. As the thickness of Gd increases, the number of Gd atoms within the material also rises, which leads to a corresponding enhancement in the contribution of Gd's magnetic moment. The total spin angular momentum in such a system accumulates from the magnetic moments of individual atoms; therefore, an increase in Gd thickness directly correlates with an increase in the overall spin angular momentum attributable to Gd.

In a Co/Gd heterostructure, the total spin angular momentum is a composite of that contributed by Co and Gd. Consequently, an increase in Gd thickness elevates the spin angular momentum of Gd, thereby altering the total spin angular momentum of the entire system. Notably, there exists a condition during the variation of Gd thickness whereby the total spin angular momenta of Co and Gd equal in magnitude but opposite in direction at a specific moment, resulting in a cancellation effect that leads to a net spin angular momentum of zero for the entire material. This zero net spin angular momentum, particularly near the spin angular momentum compensation point, minimizes the inertia associated with the motion of the domain wall, thereby facilitating high-velocity domain wall dynamics.

The phenomena of current-driven DW motion in heavy metal/ferromagnet heterostructures can be elucidated through the synergy of the SHE and DMI. The SHE engenders a distinctive torque induced by electrical currents, while the DMI plays a critical role in stabilizing chiral domain walls. The inherent symmetry of these chiral domain walls enables uniform and efficient motion. By stabilizing Néel domain walls with built-in chirality, DMI supplements the mechanisms required to elucidate the current-induced domain wall movement within heavy metal/ferromagnet systems, allowing SHE to drive these walls effectively and uniformly. This comprehensive understanding of the interactions between Gd thickness, magnetic moments, and domain wall dynamics is fundamental to advancing the field of spintronics and optimizing the efficiency of magnetic devices.

3. Conclusions

In conclusion, our investigation into the motion of domain walls (DWs) driven by current-induced SOT and external magnetic fields in rare-earth-transition metal (RE-TM) ferrimagnets has yielded significant insights. We have successfully demonstrated that the velocity of domain wall motion, propelled by current spin torque, can surpass 2 m/s under room temperature conditions. This discovery highlights the potential of Gd sub-ferromagnets as highly effective candidates for achieving rapid domain wall dynamics, which is critical for the development of next-generation spintronic devices.

The unique dynamic behavior of domain walls in various RE-TM ferromagnetic materials is underscored by our detailed analysis, revealing substantial variations in response to different material compositions and structural configurations. These findings not only enhance our understanding of the fundamental physics governing domain wall motion but also suggest practical avenues for optimizing the parameters that influence DW dynamics.

We acknowledge that the presence of the top Pt layer (5 nm) in our sample structure may contribute to the overall SOT and cannot be neglected, as it may partially counteract or modify the SOT generated by the bottom Pt and Ta layers. While the top Pt primarily serves as a capping layer, its positive spin Hall angle and relatively large thickness, exceeding the typical spin diffusion length, could attenuate spin currents from Ta before reaching the magnetic interface. Although we are unable to perform additional control experiments with thinner or omitted top Pt layers at this stage, we will study these effects in future studies.

Overall, this work lays a solid foundation for exploring the intricate interplay between microstructural properties and magnetic behavior in RE-TM ferrimagnets. Our results could serve as a catalyst for future research aimed at developing more efficient and robust spintronic devices, leveraging the advantageous characteristics of RE-TM ferromagnetic materials. This exploration paves the way for innovative applications in data storage and processing technologies, ultimately contributing to the advancement of next-generation spintronic systems.

Acknowledgements

Project supported by the Shenzhen Fundamental Research Fund (Grant No. JCYJ20210324120213037), the Basic and Applied Basic Research Foundation of Guangdong Province, China (Grant No. 2021B1515120047), the Fund from the Shenzhen Peacock Group Plan (Grant No. KQTD20180413181702403), the National Natural Science Foundation of China (Grant Nos. 12374123 and 12204396), and the 2023 SZSTI stable support scheme.

References

[1] Coey J M 2010 *Magnetism* (Cambridge University Press) p. 620
[2] Garello K, Yasin F, Hody H, Couet S, Souriau L, Sharifi S H, Swerts J, Carpenter R, Rao S, Kim W, Wu J, Sethu K K V, Pak M, Jossart N, Crotti D, Furnémont A and Kar G S 2019 *Symposium on VLSI Circuits*, June 09–14, 2019, Kyoto, Japan p. T194
[3] Grimaldi E, Krizakova V, Sala G, Yasin F, Couet S, Sankar Kar G, Garello K and Gambardella P 2020 *Nat. Nanotech.* **15** 111
[4] Sinova J, Valenzuela S O, Wunderlich J, Back C H and Jungwirth T 2015 *Rev. Mod. Phys.* **87** 1213
[5] Hoffmann A 2013 *IEEE Transactions on Magnetics* **49** 5172
[6] Yu G, Upadhyaya P, Fan Y, Alzate J G, Jiang W J, Wong K L, Takei S, Bender S, Chang L T, Jiang Y, Lang M, Tang J S, Wang Y, Tserkovnyak Y, Khalili Amiri P and Wang K L 2014 *Nat. Nanotech.* **9** 548
[7] Murray N, Liao W B, Wang T C, Chang L J, Tsai L Z, Tsai T Y, Lee S F and Pai C F 2019 *Phys. Rev. B* **100** 104441
[8] Liu Y, Zhou B and Zhu J G 2019 *Sci. Rep.* **9** 325
[9] Lau Y C, Betto D, Rode K, Coey J M and Stamenov P 2016 *Nat. Nanotech.* **11** 758
[10] Wu H, Razavi S A, Shao Q M, Li X, Wong K L, Liu Y X and Wang K L 2019 *Phys. Rev. B* **99** 184403
[11] Hansen P, Clausen C, Much G, Rosenkranz M and Witter K 1989 *J. Appl. Phys.* **66** 756
[12] Campbell I A 1972 *J. Phys. F: Metal Phys.* **2** L47
[13] Baltz V, Manchon A, Tsoi M, Moriyama T, Ono T and Tserkovnyak Y 2018 *Rev. Mod. Phys.* **90** 015005
[14] Jin S, Li J, Li Q X and Zhu J J 2024 *Chin. Phys. B* **33** 077503
[15] Usaj G, Lustemberg P and Balseiro C A 2005 *Phys. Rev. Lett.* **94** 036803
[16] Dugaev V K, Litvinov V I and Barnas J 2006 *Phys. Rev. B* **74** 224438
[17] Brey L, Fertig H A and Das Sarma S 2007 *Phys. Rev. Lett.* **99** 116802
[18] Liu Q, Liu C X, Xu C, Qi X L and Zhang S C 2009 *Phys. Rev. Lett.* **102** 156603
[19] Zhu J J, Yao D X, Zhang S C and Chang K 2011 *Phys. Rev. Lett.* **106** 097201
[20] Chang H R, Zhou J, Wang S X, Shan W Y and Xiao D 2015 *Phys. Rev. B* **92** 241103
[21] Hosseini M V and Askari M 2015 *Phys. Rev. B* **92** 224435
[22] Moore T A, Miron I M, Gaudin G, Serret G, Auffret S, Rodmacq B, Schuhl A, Pizzini S, Vogel J and Bonfim M 2008 *Appl. Phys. Lett.* **93** 262504
[23] Miron I M, Zermatten P J, Gaudin G, Auffret S, Rodmacq B and Schuhl A 2009 *Phys. Rev. Lett.* **102** 137202
[24] Miron I M, Moore T, Szambolics H, Buda-Prejbeanu L D, Auffret S, Rodmacq B, Pizzini S, Vogel J, Bonfim M, Schuhl A and Gaudin G 2011 *Nat. Mater.* **10** 419
[25] Emori S, Bono D C and Beach G S 2012 *Appl. Phys. Lett.* **101** 042405